JOURNAL OF PROPULSION AND POWER
Vol. 10, No. 2, March–April 1994

Advanced Injection and Mixing Techniques for Scramjet Combustors

David W. Bogdanoff*
Eloret Institute, Palo Alto, California 94303

Scramjet combustor fuel injection and mixing enhancement techniques are reviewed. The injection techniques include hole injection from the combustor wall, slot injection parallel to the flow, and injection from struts and the rear of ramps. Three new advanced mixing techniques are presented. The first is a combustor, curved so that buoyancy forces will aid in the penetration of the fuel across the combustor. The second is pulsation of the fuel injectors to increase penetration and mixing. A fluidic technique, a modified Hartmann-Sprenger tube, is identified as a strong candidate to generate the pulsations. The third is the injection behind pylons to allow deep penetration into the air stream. This technique is likely to produce high base pressures on the injector structure, particularly if base burning is encouraged. Curved or slanted pylons can be used to increase the recovery of fuel jet momentum. The potential of the new mixing techniques to increase scramjet engine performance is assessed.

I. Introduction

SCRAMJET operation at flight Mach numbers of 10–20 is generally believed[1,2] to require mixing and combustion at combustor inlet Mach numbers of roughly one-third the flight Mach number. The fuel, generally taken to be hydrogen, is injected and must mix and burn in the very short combustor stream residence time. Thrust is generated as relatively small differences between the large engine inlet and outlet momenta. There are inevitably frictional, shock, and other losses in the main momentum stream. Additional losses due to injection, mixing, and combustion of the fuel must be kept to a minimum and, at the same time, the most complete fuel-air mixing and fuel chemical energy release must be achieved to maximize thrust. The most important additional losses due to injection and mixing comprise shock wave losses on the fuel jets, shock wave losses and pressure and friction drag on injector mechanical structures (if any), shear layer mixing losses between fuel and air, and loss of the momentum of the fuel jets (in some configurations).

Many benchmark studies[3–11] have been done with circular hole injectors at angles of 90 deg (normal to the stream flow). Other studies[12–16] have been done with circular hole injectors at angles ranging from 0 deg (parallel to the stream flow) to 150 deg (angled upstream against the stream flow). Slot injectors[17–21] are usually oriented so that the fuel and stream velocity vectors are aligned. A number of techniques have been used to enhance the mixing of the injected flow with the stream flow. Perhaps the most basic is to use some kind of strut[22,23] or extended tube[15] so that the actual injector orifice is lifted away from the main stream wall into the body of the stream flow. Other mixing enhancement techniques include injection downstream of a rearward facing step or ramp[24–28] and the use of shock waves or expansion waves[18,20,26,27,29–32] to increase the mixing of the injected jet and the main stream.

Received Aug. 11, 1992; revision received July 3, 1993; accepted for publication July 20, 1993.

*Senior Research Scientist, 3788 Fabian Way; mailing address: NASA Ames Research Center, M/S 230-2, Moffett Field, CA 94035. Associate Fellow AIAA.

Injector types and mixing enhancement techniques are reviewed in Sec. II. Three new advanced mixing techniques are described in Sec. III and their potential to increase scramjet engine performance is assessed.

II. Injectors and Mixing Enhancement Techniques

A. Injectors

We first discuss injectors which are on the wall and do not have mechanical structure protruding into the flow. We define θ as the angle between the injector jet and the freestream. For example, $\theta = 0$ deg and $\theta = 90$ deg denote injection parallel and normal to the stream, respectively. We also introduce the following definitions: R_q is the ratio of the momentum of the injected jet to that of the adjacent freestream, and R_m is the ratio of the mass flux of the injected jet to that of the adjacent freestream. References 3–7 present data on normal circular hole injectors. References 3–5 all study a single sonic injector injecting into a Mach 4 stream. For these cases R_q ranged from 0.5–3.0 and concentration measurements were taken between $X/D = 7$ and $X/D = 200$, where D is the injector port diameter and X is distance downstream from the injector. The penetration was found to vary as $R_q^{0.5}$, $R_m^{0.54}$, or $R_q^{0.3}$ in Refs. 3–5, respectively. References 4 and 5 found the penetration (at maximum injectant concentration) to decrease between $X/D = 7$ and $X/D = 15$–40, and then to increase as X/D increases towards 200. These latter two references also found the maximum injectant concentration to vary as $(X/D)^{-0.5}$. Reference 6 studied a single sonic injector injecting into a Mach 2 stream. R_q ranged from 4.4–5.3. The height of the Mach disc was found to vary as $R_q^{0.5}$, and was about 30% lower (for a single injector) than for the multiple injector data given in Ref. 12. Stop-action photography showed the turbulent structure of the injected plume for $X/D = 0$–25. Reference 7 correlates initial penetrations (heights of Mach discs) from a number of references and calculates injector plume trajectories. The correlations are made for stream Mach numbers of 1.9–4.5 and jet Mach numbers of 1.0–2.2. The correlations are made using an effective jet back pressure p_{eb}, taken to be two-thirds of the stream pitot pressure, and the pressure at the injector throat p_j^*. The equation given is

$$\frac{Y_1}{D_j^*} = M_j^{0.25}\left(\frac{p_j^*}{p_{eb}}\right)^{0.5} \tag{1}$$

where Y_1 is the height of the Mach disc, D_j^* is the diameter of the throat of the injector, and M_j is the injector jet Mach number. The calculated integrated plume trajectories were found to approach horizontal as X/D_j^* reaches 10, and to be very similar for equal mass flows at varying injector pressures. At $X/D_j^* = 10$, the penetrations of the calculated trajectories were found to vary as $(p_{tj}/p_{t\infty})^{0.24-0.29}$, where p_{tj} is the pitot pressure of the injector jet, and $p_{t\infty}$ is the stream pitot pressure.

References 12–15 present data on angled circular hole injectors. Some key parameters for the data of these references are given in Table 1. In Table 1, S denotes the lateral spacing between the holes and N_{inj}, the number of injectors. A wide range of R_q and θ values are covered by this data. We note that the injector of Ref. 15 is above the wall, outside the boundary layer, while the injectors of Refs. 12–14 are on the wall. Also, significant differences were found to exist between the flow patterns of single and multiple injectors.[8] We will return to this point later. References 12 and 15 mainly present data on initial jet penetration, either the height of the Mach disc or the centroid of the injector gas plume. The penetration was found to vary as $R_q^{0.5}$ for both references, and as $1/(1 + \cos\theta)$ or $(\cos\theta)^{0.8}$ in Refs. 12 and 15, respectively. Reference 15 therefore finds the maximum penetration at $\theta = 90$ deg, while Ref. 12 finds the maximum penetration at the highest value of θ tested (120 deg). Increasing penetration for the data of Ref. 12 for θ increasing above 90 deg may be the result of boundary-layer separation. Reference 12 also showed increased penetration with wall blowing upstream of the injectors. References 13 and 14 measure injected gas concentrations 20–120 injector hole diameters downstream of the injectors and found the penetration at these locations to behave quite differently than the initial penetrations studied in Refs. 12 and 15. Reference 13, using five injectors, found penetration to increase with decreasing θ, being 1.5–1.6 times greater at $\theta = 30$ deg than at $\theta = 90$ deg. Reference 14, with a single injector, found penetration better at $\theta = 30$ deg than at $\theta = 15$ deg. Reference 14 also found the penetration to vary as $R_q^{0.7-0.9}$ at $X/D = 20$ and as $R_q^{0.4-0.8}$ at $X/D = 90$. From Refs. 13 and 14, it thus appears that the best penetration well downstream of the injector occurs at $\theta \simeq 30$ deg. Reference 13 compared data from single and multiple injectors. The single jet apparently initially (at $X/D \simeq 30$) penetrates less and mixes more poorly, but further downstream (at $X/D \simeq 120$), the single jet is superior on both accounts.

References 8–11 present data on tandem normal circular hole injectors. In the work of Refs. 8–10 there are two equally sized injector holes downstream of a rearward facing step. Time average and rms velocity data and injectant concentration data were obtained using laser-based techniques. The path of the injectant plume and the decay of the injectant concentration were determined. In the work of Ref. 11 there are five injector holes with diameters increasing in the downstream direction. No concentration-based penetration data are available from Ref. 11. With tandem jets, one may argue that an upstream jet can be viewed as creating streamwise vorticity which then carries the injected gas of downstream jets further into the main stream. It remains to be demonstrated whether the penetration of tandem jets is any better than that achievable by combining all of the jet array into a single, larger jet.

Reference 16 studied angled circular hole injectors ($\theta = 15$ and 30 deg) which could be yawed at angles up to 28 deg with respect to the mainstream. The yaw will produce added streamwise vorticity in the flow. Well downstream of the injectors, yaw was found to increase the lateral spreading of the injected gas by 10–30%.

References 17–21 studied slot injection parallel to the main stream. For all cases the parallel injection was at the wall. The freestream Mach numbers varied from 2 to 3 and the freestream total temperature was near 300 K for Refs. 17, 18, and 21, and the freestream static temperature was ~1300 K for Refs. 19 and 20. The parallel injection was subsonic air for Ref. 17, Mach 1.7 air for Refs. 18 and 21, and Mach 1 hydrogen for Refs. 19 and 20. The apparatus of Ref. 21 had, in addition to a parallel injection slot, 11 tubes normal to the flow, downstream of the slot and spanning the slot height. Injection normal to the freestream flow could be made through these tubes. Tests were run with no normal injection and with injection of air at Mach numbers of 1.0 and 2.2. With parallel injection, theoretically the full momentum of the injected gas is available to add to the main stream. For the geometries of Refs. 17–21, the thin, high-gradient boundary layer at the wall downstream of the slot may result in significant jet momentum losses. In general, these experiments showed rather poor mixing. Mixing was improved by the impingement of oblique shocks[18,20] on the jets and the addition of normal injection.[21]

The second main class of injectors has mechanical structures of various sorts which lift the injector ports out into the mainstream. Much improved penetration and mixing can be achieved in this way at the cost of additional momentum losses due to the mechanical structure. These losses comprise pressure and friction drag forces on the structure and additional shock and shear layer losses due to the structure. References 22 and 23 study injection from jets on struts entirely spanning the stream. The angled circular hole injector of Ref. 15 (a simple bent tube) is an example of an injector "strut" which does not extend completely across the stream. Estimates made of the momentum loss due to pressure drag forces on these struts show that these losses can be very substantial compared to representative estimated engine thrusts. Injection can also be at the downstream end of a ramp.[24–28] We will consider this type of injector in the following section on mixing enhancement.

B. Mixing Enhancement

A number of the theoretical and experimental studies[18,20,26,27,29–32] have investigated the effect of passing the injected jets through shock waves or expansion wave systems. A large fraction of these studies show substantial increases in mixing due to the addition of shock or expansion waves. Differential acceleration of different density gases by wave systems will produce baroclinic torques which will, in turn, produce vorticity and increase mixing. In two-dimensional flows, the additional vorticity can only be in the spanwise direction; in three-dimensional flows (i.e., with circular jets), additional streamwise vorticity will be created by the waves.[27,31] On two-dimensional interfaces or with two-dimensional jets, increased velocity differences due to wave systems will increase the growth rates of the Kelvin-Helmholtz instability. Curvature of the interface due to wave systems can also allow curvature-induced Rayleigh-Taylor[29,30] and Taylor-Goertler[33] instabilities to occur. Acceleration of an interface normal to itself by expansion waves or shock waves can produce the Kelvin-

Table 1 Key parameters for Refs. 12–15 for injection at an angle to the stream

Reference	Injector location	N_{inj}	S/D	Freestream Mach no.	R_q	θ, deg
12	On wall	Row of injectors	3.2–10.4	0.6, 2, 3	0.68–11.3	60–120
13	On wall	5	6.23	4	1.0	30–90
14	On wall	1	—	3	0.27–3.1	15–30
15	Above wall	1	—	2.8	4.1–8.2	30–150

Helmholtz or Richtmyer-Meshkov instabilities,[30,34,35] respectively. Thus, there are a number of mechanisms by which shock or expansion waves can increase mixing between the jets and the mainstream.

Injection at the downstream end of ramps is studied in Refs. 24–28. Figures 1a–1c show the ramp geometries of Refs. 24, 26, and 28, Ref. 25 and Ref. 27, respectively. In Fig. 1, *FS* denotes freestream flow, *I*, injector jet flow, *S*, shock wave and *E*, expansion fan. In the rear views, the dense hatching denotes the injector port. The second shock in Fig. 1a is assumed to be reflected from a top wall which is not shown. In Refs. 24–26 and 28, both swept and unswept ramps were studied. Swept and unswept ramps look identical in the side views. For unswept ramps, the corners A and B remain parallel as one moves upstream from the injector port location. For swept ramps, these corners spread outwards, as shown in the rear views. For the swept ramps, the sweep angle is ~10 deg. References 24–26 each make comparisons of swept vs unswept ramp injectors and find that greater streamwise vorticity and better mixing are obtained with swept ramp injectors. However, larger momentum losses are found[25] with the swept ramps. The ramp injectors of Refs. 25 and 27, in contrast to those of Refs. 24, 26, and 28, have a wall geometry which produces a strong oblique shock directly at the injector port. This shock wave will produce baroclinic torques and generate streamwise vorticity in the region of the main stream-jet boundary (if a density difference exists), and hence, improve mixing.[27]

III. New Advanced Mixing Techniques

In this section, three new advanced mixing techniques are presented and preliminary assessments are made of the potential which they offer for increases in scramjet engine performance.

A. Curved Combustor

Figure 2 shows sketches of two scramjet engines. These sketches are schematic only and do not represent actual candidate geometries. The fuel injector locations are denoted by *I*. A conventional straight combustor is shown in Fig. 2a. The proposed new concept is to curve the combustor, as shown in Fig. 2b, so that buoyancy forces in the accelerating reference system of the curved main flow will tend to carry the fuel plume from the injector across the combustor, ensuring good penetration and mixing without having large high-drag injector struts in the flow. This concept is a development from earlier work showing mixing enhancement due to shock or expansion waves[18,20,26,27,29–32] (see Sec. II.B.).

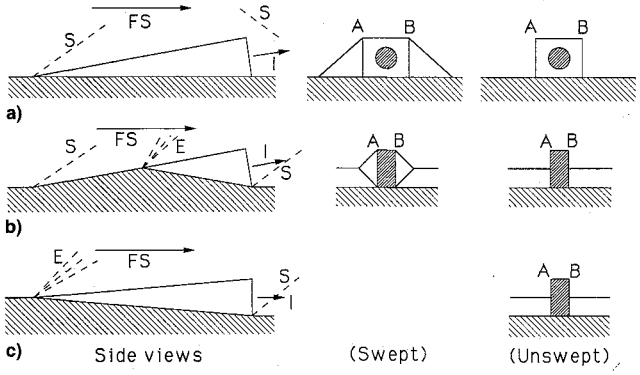

Fig. 1 ***FS*** **denotes freestream flow,** ***I*****, fuel jet flow,** ***S*****, shock waves, and** ***E*****, expansion wave systems. Dense hatching in rear views denotes the injector port. See text for discussion of letters A and B: a) ramp injector geometry from Refs. 24, 26, and 28—wall adjacent to ramp is flat; b) ramp injector geometry from Ref. 25—wall adjacent to ramp deflects towards flow, then away from flow, and finally towards flow again at injection port; and c) ramp injector geometry from Ref. 27—wall adjacent to ramp deflects away from flow and then towards flow at injector port.**

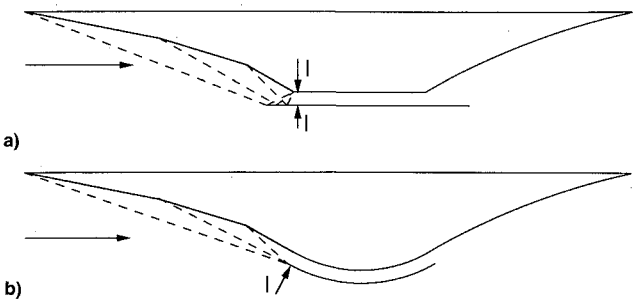

Fig. 2 Sketches of scramjet engines with a) straight and b) curved combustors. Fuel injector locations are denoted by *I* and diffuser shocks are shown dashed. Geometries and shock locations are conceptual and schematic only.

The density differences necessary to drive the fuel across the combustor stem from the low molecular weights of the fuel and combustion products and the heating due to combustion. We will examine briefly the buoyancy driven acceleration of a fuel plume of a different density than the ambient gas. Let ρ be the density of the plume, ρ_0 the density of the surrounding ambient gas, and define $\zeta = \rho/\rho_0$. To get R_a, the acceleration of the plume (neglecting viscous effects) divided by the acceleration of the local reference system, we must consider the acceleration of the plume gas plus the acceleration of the ambient gas surrounding the plume. The acceleration of the latter gas produces an "additional apparent mass" effect, which is discussed for an infinite circular cylinder in Hunsaker and Rightmire.[36] For the circular cylinder, the additional apparent mass is equal to (volume of cylinder) $\times$ ρ_0. From the solution for the flow over a sphere given in Anderson,[37] a few pages of algebra suffices to show that, for a sphere, the additional apparent mass is equal to 0.375 $\times$ (volume of sphere) $\times$ ρ_0. The total mass (buoyant gas + additional apparent mass from the ambient gas) to be accelerated and the buoyant force available can now readily be calculated as functions of ζ for cylindrical and spherical buoyant bodies, yielding R_a as functions of ζ. For a cylinder, $R_a = (1 - \zeta)/(1 + \zeta)$, and for a sphere, $R_a = (1 - \zeta)/(0.375 + \zeta)$. The values of R_a differ for cylinders and spheres since the additional apparent masses are proportional to different fractions of the buoyant volume for the two geometries. Spheres always have the greater R_a values; e.g., for $\zeta = 0.5$, for spheres $R_a = 0.571$, while for cylinders, $R_a = 0.333$. Thus, it would seem to be beneficial, on this account, to break up the fuel plume. We will return to this point in the following section.

Reference 1 gives conditions in a representative hydrogen fueled scramjet combustor at the inlet, exit, and fuel injector throat. We consider the case at Mach 15 with a fuel equivalence ratio (ER) of 1.0. The combustor inlet conditions are, pressure = 0.568×10^6 dyne/cm^2, temperature = 1908 K, Mach number = 5.189, and velocity = 4.34×10^5 cm/s. Based on possible material limitations, we take the fuel stagnation temperature to be 1000 K, rather than 1667 K as given in Ref. 1. For these conditions, the density of pure unburned fuel, after expansion to the combustor ambient pressure, can readily be estimated to be $0.46\rho_0$, where ρ_0 is taken here to be the density of the combustor inlet air. From the combustor exit temperature given in Ref. 1 for ER = 1, the density of a combustion products plume at ER = 1 can be estimated to be 0.47 times that of the combustor inlet air at the same pressure. Hence, for this case, both pure fuel and combustion products plumes will have $\zeta \simeq 0.47$, providing substantial buoyancy driven acceleration.

For methane fuel, with molecular weight 16 g/g-mole vs 2 for hydrogen, the buoyancy forces for pure unburned fuel plumes are much less favorable. There would still be large values of ζ (up to 0.50–0.70) for methane combustion products plumes, because of the large temperature increase upon combustion. However, the use of the curved combustor con-

cept with methane (or higher hydrocarbon) fuels appears less desirable than with hydrogen fuel due to the much weaker buoyancy forces for unburned fuel plumes.

Returning to hydrogen fuel, with $\zeta \simeq 0.47$, as estimated above, R_a can be estimated from the equations given above to range from 0.36–0.63, depending upon the degree of breakup of the fuel/products plumes. If an average R_a of 0.40 can be achieved and the curved combustor deflects a total of 2.5 times its height, the fuel/products plumes will cross the combustor, based on the present simple inviscid analysis. Two factors can reduce the combustor curvature and/or the average R_a value required below those values given above using the present model. First, the injectors (even if on the wall) will presumably achieve some penetration on their own, so a full crossing of the combustor by the fuel/products plumes, driven only by buoyancy effects, is not required. Second, fuel injection could begin somewhat upstream of the combustor proper. If only relatively small amounts of hydrogen combustion take place "early," such injection may produce little reduction in engine performance.

With a curved combustor, there are concerns about nonuniform wall heating, momentum loss and the generation of shock waves, and the attendent loss of stagnation pressure. To assess the severity of these effects, a two-dimensional inviscid planar CFD solution was computed for a curved combustor (without fuel injection). The inlet conditions were those given in Ref. 1 for Mach 15. The gas was taken to be calorically and volumetrically perfect with a molecular weight of 28.84 g/g-mole and a specific heat ratio of 1.4. The combustor channel is comprised of two circular arcs with 20-deg included angle, inner radius 425 cm, and height 10 cm. The length/height ratio of the channel is 15, and the channel deflects, over its length, ~2.75 times its height. The gridding used was 50 × 100, with 100 cells in the streamwise direction.

The CFD solution shows a series of continuous expansion and compression wave systems, but no shock waves, very little stagnation pressure loss, and a momentum loss of 0.28% of the inlet stream momentum. As expected, due to the flow curvature, there are substantial density gradients in the height direction. The density at the outer wall averages about 1.3–1.4 times the mean value, with maximum densities of 1.5–1.6 times the mean value. At the inner wall, the density averages 0.7–0.8 times the mean value, with minimum densities of ~0.5 times the mean value. Heating would be expected to be increased at the outer wall and decreased at the inner wall roughly in proportion to these densities. Clearly, attention must be paid to the wave systems and density variations which would occur in a curved combustor, but our preliminary CFD calculations do not show any very bad flow patterns which would weigh heavily against the curved combustor concept. It is also likely that combustor wall profiles more sophisticated than simple circular arcs could produce some reduction in the strengths of the wave systems and the magnitudes of the momentum loss and density variations. For example, supersonic flow can be turned in symmetric elbows and turbine blades[38] which, for inviscid flow, would have zero momentum and stagnation pressure losses.

B. Pulsating Injectors

It is well known that applying pulsation to subsonic jets can produce large increases in entrainment and penetration.[39,40] It is proposed here to rapidly pulse scramjet fuel injectors to improve mixing and penetration. (Also, breaking up the fuel jet could cause an increase in the jet penetration due to the buoyancy effect described in the previous section, if this technique were used.) The question arises as to what techniques would be suitable to pulsate the jet. The pulsation device must be compact, robust (to withstand temperatures of ~1000 K), and produce rapid, intense pulsations. The fuel jet flow should be reduced to near zero at the pressure minima.

It seems unlikely that mechanical pulsation devices could produce frequencies fast enough to pulse the jet each time it travels a small number (e.g., 2–3) of diameters. (It would also be difficult to make such devices survive the high-temperature environment.) By analogy with the subsonic jet experiments,[39,40] such rapid pulsing would likely be necessary to attempt to break up the jet and increase the mixing. Slower pulsing would merely produce a quasisteady jet with a periodically varying flow rate—this would be expected to produce little increase in mixing. Hence, it seems likely that fluidic techniques would be required to pulse the jet. Many fluidic oscillator techniques, e.g., the cylindrical resonant cavity technique[41] and the beam deflection amplifier with feedback technique,[42] have the disadvantages of producing low amplitude (and in some cases, low frequency) oscillations and require large, bulky flow passages. The Hartmann-Sprenger (H.-S.) tube,[43–48] in constrast, is compact and produces very large amplitude, rapid pulsations. Peak-to-peak oscillation amplitudes observed[43–46] in H.-S. tubes are roughly equal to the stagnation pressure in the exciting jet. Hence, we consider the H.-S. tube to be a strong (though not necessarily the only) candidate to pulse the fuel jets.

A possible injector geometry using an annular H.-S. tube is shown schematically in Fig. 3. (We note that the Hartmann-Sprenger tube was mentioned in Ref. 49, but as applied to the production of oscillatory shock waves and not to fuel injectors.) Below, we make an estimate of how finely the H.-S. geometry of Fig. 3 can break up the jet. We assume that the length of the H.-S. tube is 1.4 cm. To the same scale the nozzle throat and exit diameters are 2 and 4 cm, respectively. We take the fuel to be ideal hydrogen at a stagnation temperature of 1000 K. Using the open-closed organ pipe formula for the H.-S. tube and assuming it to operate at 1000 K, its frequency is calculated to be 43 kHz. Using standard isentropic flow tables, the nozzle exit velocity can be calculated to be 4.3 km/s. Hence, the injected fuel plume moves about 2.5 nozzle exit diameters per cycle. This is sufficiently fast to break the plume up if, of course, the pulsation of the flow rate has sufficient amplitude.

Two important points must be made here. First, Fig. 3 is conceptual only; obviously a number of geometries and operating conditions would have to be tested and the most suitable of both found. Second, it is well known that very high temperatures can be produced in H.-S. tubes.[43–48] This could be very detrimental to the survivability of such a device in the scramjet combustor environment. However, we note from the same references that the temperatures reached are very much dependent on the geometry and operating conditions of the H.-S. tubes. Also, many of the H.-S. tube geometries and operating conditions described have been developed specifically to produce these high temperatures. In the course of developing a H.-S. tube/nozzle geometry suitable for scramjet combustor injectors, emphasis would be placed on producing

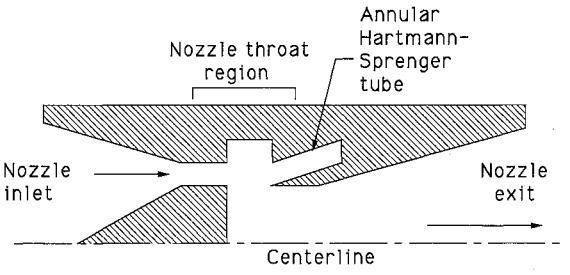

Fig. 3 Hydrogen fuel injector nozzle concept employing an annular Hartmann-Sprenger tube to produce rapidly pulsating flows. Nozzle is designed for Mach 3 exit flows.

strong pulsations while limiting the temperatures reached to values acceptable based on materials considerations. The data given in Refs. 43–48 suggest that it may well be possible to achieve this goal.

C. Pylon Injection (Injection Behind Pylons)

The basic concept is shown, for a 90-deg injector, in Fig. 4. The pylon allows the fuel jet to penetrate deeply into the combustor. This concept is related to the ramp injectors,[24–28] but, in part, has some advantages since the fuel does not pass through the protruding injector structure. For simplicity, we have shown a circular injector port in Fig. 8, but by elongating the port in the direction of the stream flow, the same size pylon could be made to serve for an injector with greater mass flow. Particularly with an elongated injection port, the pylon can be likely be made smaller than the corresponding ramp[24–28] injectors since the fuel passage is inside the ramp in the latter cases. Also, the rear (base) pressure on the pylon is likely to be larger than that for ramp injectors due to the presence of an adjacent parallel jet and possibly base combustion. (References 50 and 51 show that large reductions in the base drag of projectiles can be achieved using base burning.) Hence, the drag of the pylon is likely to be considerably less than that for the ramp of ramp injectors. The 90-deg injector shown in Fig. 4 has the disadvantage that the fuel jet momentum will be totally lost. More viable pylon injector concepts are shown in Figs. 5a and 5b. Here, the pylons are tilted or curved to allow partial recovery of the fuel jet momentum. The pressure on the base of the curved pylon will be increased due to the turning of the jet.

Two additional possible refinements of the pylon injector will now be presented (as applied to a 90-deg injector). Figures 5c and 5d show the concept of the partial trapping of the fuel jet in the recessed rear of the pylon. This concept would help to resist the tendency of the jet to be deflected away from the rear of the pylon by the mainstream flow and consequent reduction of jet penetration. Figure 6 shows the tapered pylon concept. The tapering, which need not be linear, would be adjusted to optimize the vertical distribution of fuel in the combustor. For simplicity the above concepts were shown applied singly to a 90-deg injector, but they could very well be applied to tilted or curved injectors and/or combined with each other.

The three new advanced mixing techniques presented in this section could be used together in the same combustor to maximize combustor performance.

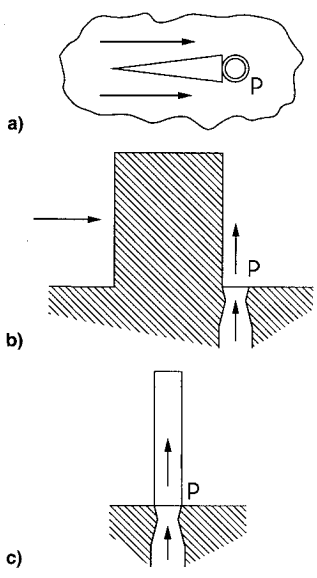

Fig. 4 Basic pylon injector concept: a) top view, b) side view, and c) rear view. *P* is the injector port.

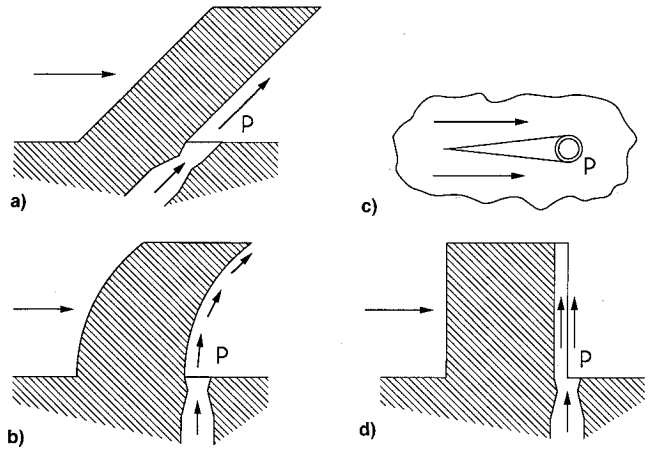

Fig. 5 Pylon injector with curved rear to trap the injector jet: a) tilted pylon injector, b) curved pylon injector, c) side view (section), and d) top view.

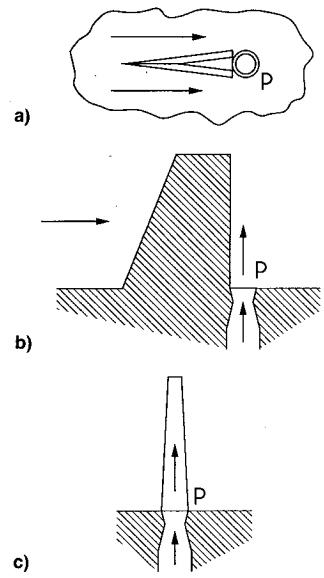

Fig. 6 Three views of tapered pylon injector concept: a) top view, b) side view (section), and c) rear view (section).

D. Performance Assessment of Proposed Advanced Mixing Concepts

At this point, an assessment is made of the potential for scramjet engine performance increases offered by the advanced mixing concepts presented in the three preceding sections. We consider as representative the combustor inlet conditions for flight at Mach 15 given in Ref. 1. These are 1) pressure = 0.568×10^5 dyne/cm^2, 2) temperature = 1908 K, 3) Mach number = 5.19, and 4) velocity = 4.34×10^5 cm/s. For these conditions, using a simple five species air equilibrium solver, we calculate that the molecular weight = 28.8 g/g-mole and the specific heat ratio = 1.300. For a fuel equivalence ratio of 1.0 and a full kinetic nozzle expansion, Ref. 1 gives calculated thrust coefficients (C_T) of ~0.117. C_T is calculated[52] as the thrust divided by the freestream dynamic pressure and the engine inlet area. Now, since we are going to assess the loss in stream momentum in passing through the combustor, we would rather deal with a thrust coefficient based on the freestream dynamic pressure and the captured stream area at the freestream condition. For flight at Mach 15, Ref. 1 gives the ratio of captured area to engine inlet area as 0.7. Hence, defining a new thrust coefficient C_T' as thrust divided by freestream dynamic pressure divided by capture area at the freestream condition, we have $C_T' = 0.117/0.7 = 0.167$. This result is for a hydrogen fuel total temperature of 1667 K. Based on material considerations, we will consider,

instead, a fuel total temperature of 1000 K. Using a scramjet engine cycle solver described in Ref. 53, we have estimated that at C_T' will drop by ~0.02 for a fuel total temperature drop from 1667 to 1000 K. Hence, for the following discussion, we will take C_T' to be 0.147 for a fuel injection total temperature of 1000 K.

The first comparison will be between a curved combustor with injectors on the outer wall, not projecting into the stream, and a benchmark straight combustor with representative, well-documented injectors with structures protruding into the stream. We will make the assumption that equivalent combustion efficiencies can be achieved using these two combustors, and will estimate the momentum loss penalty due to the intrusive injector structures in the straight combustor. (Detailed CFD analyses of these flows for these cases would undoubtedly be of great interest, but could easily comprise several separate papers and are far beyond the scope of the present article.)

We consider the swept ramp geometry investigated in Refs. 24, 26, and 28. In Ref. 24, tests were made with actual hydrogen fuel combustion in a hot, vitiated air facility with oxygen replenishment. For equivalence ratios of 1.0, combustion efficiencies were estimated to be 50–60%. In Ref. 24, the ramp deflection angle is 10.3 deg, and from the ramp dimensions given therein, the fraction of the channel blocked by the ramp exits is 11.5%. However, the 10.3-deg faces of the ramps occupy 22.3% of the channel flow area. Reference 54 gives equations permitting one to solve the oblique shock problem for given values of upstream Mach number, deflection angle, and gas specific heat ratio. For the combustor inlet flow of Ref. 1 for a flight Mach number of 15, and a ramp deflection angle of 10.3 deg, the pressure and Mach number behind the oblique shock may readily be calculated to be 0.174 × (stream dynamic pressure) and 4.29, respectively. Assuming the pressure to be uniform on the 10.3-deg surface of the ramps, and zero on the rear and side surfaces of the ramps, the force on the ramps can easily be shown to correspond to a decrease in C_T' of 0.0353, a very significant fraction of the total available C_T'. Based on the Mach angle after the ramp oblique shock, 91% of the 10.3-deg surfaces of the ramps will be at the full pressure downstream of the shock. However, there will be some pressure recovery on the side and rear surfaces of the ramps. Hence, we make the rough estimate that the effective loss of C_T' due to pressure forces on the ramp will be two-thirds of the value estimated above or 0.0236. This is 16% of the total available C_T', still a very significant loss.

The geometry of the combustor channel analyzed above, looking upstream from a position downstream of the injectors, is shown in Fig. 7a. The penetration data for swept ramp and similar injectors given in Refs. 25–28 and the relatively low combustor efficiencies estimated in Ref. 24 suggest that the injector configuration of Fig. 7a may not provide sufficient penetration and mixing of the fuel jets. If additional ramp injectors were provided, as shown in Fig. 7b, penetration, mixing, and combustor efficiency are likely to be significantly enhanced. However, as a first estimate, the effective loss of C_T' due to pressure forces on the ramps would now be doubled, to 32% of the total available C_T', a very large loss. If, as postulated, the curved combustor could achieve equivalent mixing and combustion efficiencies (due to buoyancy effects) without drag forces on injector structures protruding into the stream, substantial increases in C_T' could be achieved. (We note that the loss in momentum calculated in Sec. III.A. for the curved combustor corresponds to only 3.5% of the total available C_T', and this could perhaps be further reduced by optimization of the curved combustor shape.)

For an assessment of the performance of injection behind pylons, we use the same ramp injector combustor geometries discussed above as the benchmark. The combustor inlet conditions are again those from Ref. 1, given at the beginning of this section. The fuel total temperature is again taken to be 1000 K, and the fuel total pressure is taken from Ref. 1 as 4.41×10^7 dyne/cm^2 (for a fuel equivalence ratio of 1.0). The pylon geometry considered is shown in Fig. 8. The height of the pylon is taken to be equal to that of the ramp injector, and it is considered to stand in the same combustor channel used with the ramp injector. The pylon and the injection channel are raked back at 30 deg to the flow direction, and the fuel is fully expanded to the combustor static pressure upstream of the pylons before injection. This corresponds to injection at Mach 3.51. For the fuel equivalence ratio of 1.0, the area of the fully expanded fuel jet can easily be calculated to be 0.0605 times the combustor channel area. In Fig. 8, we have rather arbitrarily taken the height of the fuel channel (perpendicular to the fuel flow) to be equal to the height of the pylon, and have taken the half-angle sweep of the pylon (viewed normal to the end of the pylon) as equal to the ramp deflection angle of the ramp injectors. We assume that the same mixing and combustion efficiencies can be obtained using the pylon injection technique or ramp injectors.

The main advantage of the pylon technique is that the pylon forward drag surfaces only obstruct 0.0605 of the channel area vs 0.2229 of the channel area for the 10.3-deg deflection surface of the ramp injectors. The estimated pressure on the forward drag surfaces of the pylons is essentially equal to that on the 10.3-deg surface of the ramps. There will be some reduction in the average pressure on the forward surfaces of the pylons due to expansion waves emanating from the top of the pylons. To estimate the reduction in C_T' due to pressure drag forces on the pylons, we make the same assumption used to estimate this reduction for the ramp injectors. This is, the effective pressure difference between the forward and rear surfaces of the pylon is taken to be equal to two-thirds of the pressure calculated for the forward surfaces with no allowance made for the relieving effects of expansion waves. The result of this calculation is that, for injectors on one side only of the combustor channel, the reduction in C_T' due to pressure drag

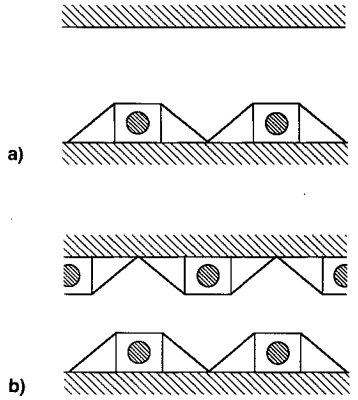

Fig. 7 Rear view of swept ramp injectors in combustor channel: a) as in experimental work of Ref. 24 and b) with twice as many injectors which may be required for good mixing and high combustion efficiency. See text, Sec. III.D.

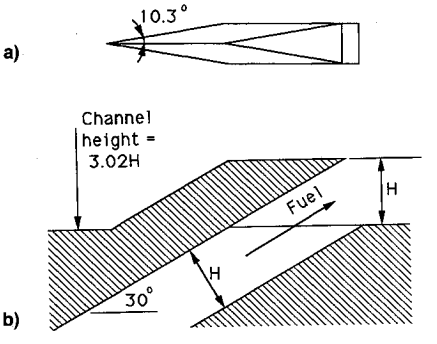

Fig. 8 Injection behind pylon: a) top view and b) side view (section). This sketch used in the assessment of the performance of the pylon injection technique, Sec. III.D.

on the injectors is 4.4% of the available C_T' for the pylon injection technique vs 16% for the ramp injectors, a very significant improvement. If, as discussed previously for the curved combustor channel, it is required to double the number of injectors to assure good mixing and combustion efficiency, these numbers would increase to 8.8 and 32%, and the difference between the ramp and pylon injection technique becomes even more significant.

In the above comparison of the ramp and pylon injection techniques, we have ignored the question of differences between the degree of recovery of fuel jet momentum for the two techniques. The angle of injection for the ramp injectors (10.3 deg) is more favorable than that for pylon injection (30 deg). On the other hand, the fuel jet expansion is more complete (to Mach 3.51) for pylon injection than for ramp injection (to Mach 1.7). The latter favors pylon injection. The overall effect is to slightly favor pylon injection. It may be argued that the ramp injector fuel channels could be altered to provide expansion of the fuel to Mach 3.51 and still to have the favorable ramp injector injection angle. On the other hand, it may also be argued that the pylon injectors and fuel channels could perhaps be raked downstream at a angle smaller than 30 deg to the flow direction, or that curved pylons (e.g., see Fig. 5b) could be used to allow improved recovery of the fuel jet momentum. From the current discussion, it appears that the degree of fuel jet momentum recovery is roughly equal for the ramp and pylon injection techniques. Hence, in the preceding paragraph, this rough equality was implicitly assumed.

We now make an assessment of the performance gains which might be achieved using the pulsating injector technique. The performance gains are assumed to be made because better mixing and higher combustion efficiencies would be obtained with pulsating injectors. As mentioned earlier, in the experimental investigation of Ref. 24, using ramp injectors at equivalence ratios of 1.0, combustion efficiencies were estimated to be 50–60%. Higher combustion efficiencies would be desirable. Using the scramjet engine cycle solver described in Ref. 53, we have calculated that for flight at Mach 15 and a fuel equivalence ratio of 1.0, C_T' increases by ~0.03 for each 20% increase in combustion efficiency. Thus, if the use of a pulsating injector can increase the combustion efficiency from 60% to, say, 80%, C_T' would be increased by 0.03. Starting from our baseline C_T' value of 0.147, this would represent a 20% increase in C_T', a very significant improvement.

The following important point must be made regarding the preceding discussion. It is not intended above to in any way imply that the new injector/mixing concepts necessarily will exhibit better performance than a straight combustor with ramp injectors—the latter injectors are proven and are known to be quite effective. Furthermore, the flows being compared are very complex—they are three-dimensional, unsteady, turbulent, and contain separated flow regions—hence, the actual performance of the new injector/mixing concepts (e.g., regarding mixing and combustion efficiency) are very difficult to predict. The new injector/mixing concepts look sufficiently good when compared to a benchmark ramp injector combustor, using simple but reasonably constructed analyses, it is argued that further investigation is warranted.

IV. Conclusions

A number of fuel injection and mixing enhancement techniques, as applied to scramjet combustors, have been briefly reviewed. The injection techniques include normal hole injection, angled hole injection, tandem normal hole injection, and yawed hole injection from the combustor wall, slot injection parallel to the flow, injection from struts spanning or not spanning the stream, and injection from the rear of ramps. The mixing enhancement techniques include the use of shock waves and expansion waves, rearward facing steps, and variations of the geometry of ramp injectors.

Three new advanced mixing techniques were presented. The first was a combustor, curved so that buoyancy forces will aid in the penetration of the fuel across the combustor. The effect of two fuel plume geometries was analyzed. The curvature and combustor length required for the fuel to cross the combustor were assessed. The second was pulsation of the fuel injectors to increase penetration and mixing. A fluidic technique, a modified Hartmann-Sprenger tube, was identified as a strong candidate to generate the pulsations. The Hartmann-Sprenger tube must be optimized to produce strong pulsations without producing excessive heat transfer. The third was the injection behind pylons to allow deep penetration into the airstream. This technique is likely to produce high base pressures on the injector structure. Curved or slanted pylons can be used to increase the recovery of fuel jet momentum. Tapered pylons can be used to optimize fuel distribution. Control of the fuel jet can be improved by partially trapping it in the curved rear of the pylon. It may also be possible to increase the base pressure on the pylon by deliberately diverting a fraction of the fuel for base burning on the pylon.

A preliminary assessment of the potential of the three new mixing techniques to increase scramjet engine performance has been made. Combustors using the new techniques were compared with a benchmark combustor with swept ramp injectors. In these assessments, the new mixing techniques looked sufficiently good compared to the benchmark case to warrant further investigation.

Acknowledgments

This work was supported by the Eloret Institute under Grant NCC2-487. The CFD solution for the curved combustor was computed by S. Polsky of the Eloret Institute.

References

[1]Billig, F. S., "Current Problems in Nonequilibrium Gas Dynamics—Scramjet Engines," AIAA Professional Study Seminar on Nonequilibrium Gas Dynamics, Honolulu, HI, June 1987, Table II.2.

[2]Swithenbank, J., Ewan, B. C. R., Chin, S. B., Shao, L., and Wu, Y., "Mixing Power Concepts in Scramjet Combustor Design," Combustion Workshop, NASA Langley Research Center, Hampton, VA, Oct. 1989, p. 16, Figs. 21, 22, and 24.

[3]Torrence, M. G., "Concentration Measurements of an Injected Gas in a Supersonic Stream," NASA TN D-3860, April 1967.

[4]Torrence, M. G., "Effect of Injectant Molecular Weight on Mixing of a Normal Jet in a Mach 4 Air Stream," NASA TN D-6061, Jan. 1971.

[5]Rogers, R. C., "A Study of the Mixing of Hydrogen Injected Normal to a Supersonic Airstream," NASA TN D-6114, March 1971.

[6]Hermanson, J. C., and Winter, M., "Imaging of a Tranverse, Sonic Jet in Supersonic Flow," AIAA/ASME 27th Joint Propulsion Conf., Sacramento, CA, June 1991.

[7]Billig, F. S., Orth, R. C., and Lasky, M., "A Unified Analysis of Gaseous Jet Penetration," *AIAA Journal*, Vol. 9, June 1971, pp. 1048–1058.

[8]Fletcher, D. G., and McDaniel, J. C., "Quantitative Characteristics of a Nonreacting, Supersonic Combustor Using Laser-Induced Iodine Fluorescence," AIAA Paper 89-2565, July 1989.

[9]Abbitt, J. D., III, Hartfield, R. J., Jr., and McDaniel, J. C., "Mole-Fraction Imaging of Transverse Injection in a Ducted Supersonic Flow," *AIAA Journal*, Vol. 29, March 1991, pp. 431–435.

[10]McDaniel, J. C., Fletcher, D. G., Hartfield, R. J., Jr., and Hollo, S. D., "Staged Tranverse Injection into Mach 2 Flow Behind a Rearward-Facing Step: A 3-D Compressible Test Case for Hypersonic Code Validation," AIAA 3rd International Aerospace Planes Conf., Orlando, FL, Dec. 1991.

[11]Clement, P., and Rodriguez, C., "Shock Wave Structure and Penetration Height in Transverse Jets," AIAA Paper 89-0841, Jan. 1989.

[12]Cohen, L. S., Coulter, L. J., and Egan, W. J., Jr., "Penetration and Mixing of Multiple Gas Jets Subject to a Cross Flow," *AIAA Journal*, Vol. 9, April 1971, pp. 718–724.

[13]McClinton, C. R., "The Effect of Injection Angle on the Interaction Between Sonic Secondary Jets and a Supersonic Free Stream,"

NASA TN D-6669, Feb. 1972.

[14]Mays, R. B., Thomas, R. H., and Schetz, J. A., "Low Angle Injection into a Supersonic Flow," AIAA Paper 89-2461, July 1989.

[15]Lee, R. E., and Linevsky, M. J., "Shadowgraph Studies of Angular Injection of a Sonic Jet into a Mach 2.8 Supersonic Flow," AIAA Paper 90-1618, June 1990.

[16]Fuller, E. J., Thomas, R. H., and Schetz, J. A., "Effects of Yaw on Low Angle Injection into a Supersonic Flow," AIAA Paper 91-0014, Jan. 1991.

[17]Schetz, J. A., and Gilreath, H. E., "Tangential Slot Injection in Supersonic Flow," *AIAA Journal*, Vol. 5, Dec. 1967, pp. 2149–2154.

[18]Hyde, C. R., Smith, B. R., Schetz, J. A., and Walker, D. A., "Turbulence Measurements for Heated Gas Slot Injection in Supersonic Flow," *AIAA Journal*, Vol. 28, Sept. 1990, pp. 1605–1614.

[19]Burrows, M. C., and Kurkov, A. P., "Analytical and Experimental Study of Supersonic Combustion of Hydrogen in a Vitiated Airstream," NASA TM X-2828, Sept. 1973.

[20]Domel, N. D., and Thompson, D. S., "A Two-Dimensional Numerical Simulation of Shock-Enhanced Mixing in a Rectangular Scramjet Flowfield with Parallel Hydrogen Injection," AIAA Paper 91-0377, Jan. 1991.

[21]King, P. S., Thomas, R. H., and Schetz, J. A., "Combined Tangential-Normal Injection Into a Supersonic Flow," AIAA Paper 89-0622, Jan. 1989.

[22]McClinton, C. R., Torrence, M. G., Gooderum, P. B., and Young, I. G., "Nonreactive Mixing Study of a Scramjet Swept-Strut Fuel Injector," NASA TN D-8069, Dec. 1967.

[23]Adelman, H. G., Cambier, J.-L., and Menees, G. P., "Experimental and Analytical Investigations of Wave Enhanced Supersonic Combustors," AIAA Paper 89-2787, July 1989.

[24]Northam, G. B., Greenberg, I., and Byington, C. S., "Evaluation of Parallel Injector Configurations for Supersonic Combustion," AIAA Paper 89-2525, July 1989.

[25]Drummond, J. P., Carpenter, M. H., Riggins, D. W., and Adams, M. S., "Mixing Enhancement in a Supersonic Combustor," AIAA Paper 89-2794, July 1989.

[26]Davis, D. O., and Hingst, W. R., "Progress Towards Synergistic Hypermixing Nozzles," AIAA Paper 91-2264, June 1991.

[27]Waitz, I. A., Marble, F. E., and Zukoski, E. E., "An Investigation of a Contoured Wall Injector for Hypervelocity Mixing Augmentation," AIAA Paper 91-2265, June 1991.

[28]Hartfield, R. J., Jr., Hollo, S. D., and McDaniel, J. C., "Experimental Investigation of a Supersonic Swept Ramp Injector Using Laser-Induced Iodine Fluorescence," AIAA Paper 90-1518, June 1990.

[29]Shau, Y. R., and Dolling, D. S., "Experimental Study of Spreading Rate Enhancement of High Mach Number Turbulent Shear Layers," AIAA Paper 89-2458, July 1989.

[30]Li, C., Kailasanath, K., and Book, D. L., "Mixing Enhancement Due to Pressure and Density Gradients Generated by Expansion Waves in Supersonic Flows," AIAA Paper 91-0374, Jan. 1991.

[31]Drummond, J. P., "Mixing Enhancement of Reacting Parallel Jets in a Supersonic Combustor," AIAA Paper 91-1914, June 1991.

[32]Menon, S., "Shock-Wave-Induced Enhancement in Scramjet Combustors," AIAA Paper 89-0104, Jan. 1989.

[33]Wang, C., "The Effects of Curvature on Turbulent Shear Layers," Ph.D. Dissertation, California Inst. of Technology, Pasadena, CA, 1984.

[34]Richtmyer, R. D., "Taylor Instability in Shock Acceleration of Compressible Fluids," *Communications in Pure and Applied Mathematics*, Vol. 13, May 1960, pp. 297–319.

[35]Meshkov, Y. Y., "Instability of a Shock Wave Accelerated Interface Between Two Gases," NASA TT F-13,079, June 1970.

[36]Hunsaker, J. C., and Rightmire, B. G., *Engineering Applications of Fluid Dynamics*, McGraw-Hill, New York, 1947, pp. 227, 228.

[37]Anderson, J. D., Jr., *Fundamentals of Aerodynamics*, McGraw-Hill, New York, 1984, pp. 280–283.

[38]Shapiro, A. H., *The Dynamics and Thermodynamics of Compressible Fluid Flow*, Ronald, New York, 1953, pp. 504–506.

[39]Platzer, M. F., Simmons, J. M., and Bremhorst, K., "Entrainment Characteristics of Unsteady Subsonic Jets," *AIAA Journal*, Vol. 16, March 1978, pp. 282–284.

[40]Vermeulen, P. J., Chin. C.-F., and Yu, W. K., "Mixing of an Acoustically Pulsed Air Jet with a Confined Crossflow," *Journal of Propulsion and Power*, Vol. 6, No. 6, 1990, pp. 777–783.

[41]Schmidlin, A. E., and Rakowsky, E. L., "A Jet Driven Flueric Amplifier," *Advances in Fluids*, edited by F. T. Brown, American Society of Mechanical Engineers, New York, 1967, pp. 282–297.

[42]Halbach, C. R., Otsap, B. A., and Thomas, R. A., "A Pressure Insensitive Fluidic Temperature Sensor," *Advances in Fluids*, edited by F. T. Brown, American Society of Mechanical Engineers, New York, 1967, pp. 298–312.

[43]Brocher, E., and Kawahashi, M., "Wave and Thermal Phenomena in H.-S. Tubes with an Area Constriction," *Proceedings of the Fifteenth International Symposium on Shock Waves and Shock Tubes* (Berkeley, CA), July–Aug. 1985, pp. 179–185.

[44]Neemeh, R. A., and Elabdin, M. N., "Performance and Characteristics of Cylindrical Resonator Igniters," *AIAA Journal*, Vol. 29, May 1991, pp. 845–848.

[45]Sarohia, V., and Back, L. H., "Experimental Investigation of Flow and Heating in a Resonance Tube," *Journal of Fluid Mechanics*, Vol. 94, Pt. 4, 1979, pp. 649–672.

[46]Kawahashi, M., Bobone, R., and Brocher, E., "Oscillation Modes in Single-Step Hartmann-Sprenger Tubes," *Journal of the Acoustical Society of America*, Vol. 75, March 1983, pp. 780–784.

[47]Brocher, E., "Heat Transfer and Equilibrium Temperature Near the End Plate of a Hartmann-Sprenger Tube," *Proceedings of the Eleventh International Symposium on Shock Waves and Shock Tubes* (Seattle, WA), July 1977, pp. 66–73.

[48]Rakowsky, E. L., Corrado, A. P., and Marchese, V. P., "Fluidic Explosive Initiator," *Fluidics Quarterly*, Vol. 6, No. 2, 1974, pp. 13–32.

[49]Kumar, A., Bushnell, D. M., and Hussaini, M. Y., "Mixing Augmentation Technique for Hypervelocity Scramjets," *Journal of Propulsion and Power*, Vol. 5, No. 5, 1989, pp. 514–522.

[50]Strahle, W. C., Hubbart, J. E., and Walterick, R., "Base Burning Performance at Mach 3," *AIAA Journal*, Vol. 20, July 1982, pp. 986–991.

[51]Gunners, N.-E., Andersson, K., and Hellgren, R., "Base-Bleed Systems for Gun Projectiles," *Gun Propulsion Technology*, edited by L. Stiefel, Vol. 109, Progress in Astronautics and Aeronautics, AIAA, Washington, DC, 1988, pp. 537–562.

[52]Billig, F. S., "Design and Development of Single-Stage-to-Orbit Vehicles," *Johns Hopkins APL Technical Digest*, Vol. 11, Nos. 3 and 4, 1990, pp. 336–352.

[53]Menees, G. P., Adelman, H. G., Cambier, J.-L., and Bowles, J. V., "Wave Combustors for Trans-Atmospheric Vehicles," 9th International Symposium on Airbreathing Engines, Paper 11-5, Athens, Greece, Sept. 1989.

[54]Liepmann, H. W., and Roshko, A., *Elements of Gasdynamics*, Wiley, New York, 1957, pp. 85–88.